

## INVESTIGATION OF SUPERSONIC TRANSIENT LOADS IN THE T-38 1.5m × 1.5m TRISONIC WIND TUNNEL AT ŽARKOVO

Dorđe Vuković, B.Sc, Aeronautical Institute Žarkovo

### Abstract

From the first runs in the supersonic Mach number range in the new T-38 trisonic wind tunnel at Žarkovo, it was discovered that the transient loads acting on models during the starting and stopping of the supersonic flow were greater than those estimated during wind tunnel design. This severely limited the use of the wind tunnel for supersonic testing. A series of measurements was conducted to investigate the cause and nature of these loads, including the determination of minimum operating pressures of the wind tunnel, recording of transient loads for various test conditions and attempts to reduce loads using devices in the wind tunnel test section. A simple empirical method was established to normalize the transient loads with model size, and so enable estimate for future tests of other models. Based on the gained experience, the design of new support stings and wind tunnel balances with appropriate characteristics was initiated. This equipment will be able to withstand the transient loads for most model configurations, enabling, at the same time, sufficiently accurate measurements.

$P_{0min1}$	Normalized minimum start pressure
$P_{0min2}$	Normalized minimum stop pressure
$R_{Amax}$	Maximum transient axial force
$R_{Ymax}$	Maximum transient side force
$R_{Nmax}$	Maximum transient normal force
$M_{xmax}$	Maximum transient rolling moment
$M_{ymax}$	Maximum transient pitching moment
$M_{zmax}$	Maximum transient yawing moment
$S_l$	Lifting surface projected area
$S_t$	Total projected model area
$S_x$	Projected frontal model area
$S_y$	Projected profile model area
$S_z$	Projected plan model area

### The Wind Tunnel Facility

The T-38 facility<sup>(1)</sup> at the Aeronautical Institute (VTI), Žarkovo, Federal Republic of Yugoslavia, is a pressurized, blow-down wind tunnel for tests in the Mach number range 0.2 to 4.0 at Reynolds numbers up to 100 million/metre. Test section size is 1.5m × 1.5m. Stagnation pressures in the range 1.2bar to 15bar can be achieved, depending on the desired Mach number, and the available run time is 6s to 60s. The wind tunnel is equipped with a porous-walls transonic test section in which a 1.5m × 0.38m insert can be mounted for 2D wing section tests. The 3D models are normally supported by a tail sting mechanism enabling movements in pitch and roll. Mach number regulation in the subsonic and transonic speed range is performed by choke flaps and a blow-off system, while in the supersonic speed range the Mach number is set by means of a flexible nozzle.

Operation of the facility and data reduction are largely automated. A 64 channels Teledyne data acquisition and recording system (DARS) with 16 bit resolution is used. Data storage and reduction is performed by a VAX 11/780 computer.

### The Transient Loads Problem

Starting and stopping of the supersonic flow in a wind tunnel is characterized by the passage of an asymmetric, randomly developed shock wave system through the test section. It can lead to large variations of local pressures and flow direction, in which case the model tested is subjected to loads considerably greater than those experienced during steady flow conditions. These aerodynamic loads put considerable strain on models, model

### List of Symbols

$\alpha$	angle of attack
$A_{ts}$	Test section area
$A_2$	Second throat area
$\beta$	Area ratio $S_l/S_t$
$B$	Model wing span
$C_{Ax}$	Transient axial force coefficient
$C_{Ay}$	Transient lateral force coefficient
$C_{Az}$	Transient normal force coefficient
$C_{*}$	Transient force coefficient
$k_x$	Normalized transient axial force
$k_y$	Normalized transient side force
$k_z$	Normalized transient normal force
$k_l$	Normalized transient rolling moment
$k_m$	Normalized transient pitching moment
$k_n$	Normalized transient yawing moment
$L$	Model length
$M$	Mach number
$P_{atm}$	Atmospheric pressure
$P_y$	Lateral pressure difference
$P_z$	Normal (vertical) pressure difference
$P_0$	Stagnation pressure
$P'_0$	Stagnation pressure behind normal shock
$P_{0min}$	Normalized minimum operating pressure

support and measuring equipment.

This problem was recognized during the design of the wind tunnel, when an estimate<sup>(7)</sup> of supersonic transient loads was made using the 'normal-shock method'<sup>(3)</sup>. The estimated loads were compared to aerodynamic loads expected during the test conditions for models at maximum available stagnation pressure (i.e. maximum Reynolds number achievable). The conclusion was reached that the transient loads would not exceed stationary loads, and so model protection devices, such as proximity plates, would not be needed. No provision was thus made for any such devices.

Unfortunately, however, this analysis did not take into account that very few models can be tested at maximum stagnation pressure, due to stress limitations imposed on models of the usual, slender missile shape, and appropriate balances and stings which must have relatively small cross-sections.

Another drawback became apparent when the first wind tunnel commissioning runs were made, when a traversing rake used to calibrate the supersonic test section was unexpectedly broken by the transient loads at Mach 3.5, while an AGARD-B calibration model had a near escape at Mach 2.5; it was found that the minimum operating pressures of the T-38 wind tunnel were considerably higher than the design estimate<sup>(8)</sup>, and so were the transient loads, which are directly proportional to the minimum operating pressure. The increase of minimum pressure was a consequence of rather overdimensioned diffuser baffles and silencer, which were needed because of strict noise constraints (the T-38 wind tunnel is located in a residential area).

### Wind Tunnel Tests

#### Minimum Operating Pressure

In order to determine the minimum operating pressures in the supersonic Mach number range, it was decided to make measurements during the startup and shutdown phases of normal wind tunnel runs made at stagnation pressures positively higher than the expected minimum. This approach was much preferred to trial and error method of attempting wind tunnel runs at various pressures close to minimum. Measurements were made using three Kulite SVQ500 piezoresistive absolute pressure transducers and a Rosemount capacitive absolute pressure transducer. The first transducer was used to measure the stagnation pressure  $P_0$  in the settling chamber, the second one measured the test section static pressure from a port on the left sidewall, and the third transducer measured the stagnation pressure  $P'_0$  behind the shock wave of a pitot-probe in the test section. In order to assure the fast response necessary, the volume of the pneumatic leads from the measurement points to the transducers was kept to a practi-

cal minimum of about 0.3m of 0.063" tubing. Rosemount transducer was used to measure the atmospheric pressure  $P_{atm}$  (i.e. the wind tunnel diffuser exit pressure) so that startup and shutdown pressure ratios could be determined. The transducers were connected to the DARS, with sampling rates of 500Hz/channel and low pass filters set at 250Hz.

Measurements showed considerable difference between the startup and shutdown pressures: the supersonic flow established at pressures  $P_{0_{min1}}$  higher than those estimated in<sup>(8)</sup> (see Fig. 1), but after that, it could be maintained at lower pressures, down to  $P_{0_{min2}}$ , which is a situation characteristic for supersonic wind tunnels with a second throat, although the T-38 wind tunnel was not designed to have a second throat. The shutdown minimum pressures  $P_{0_{min2}}$  were near to those estimated during the wind tunnel design.

It was suggested by the wind tunnel designers that the diffuser choke flaps, normally used to set Mach number in the subsonic and transonic speed ranges could be used to form an optimum second throat and reduce the minimum pressure ratio. A series of measurements was thus executed with various settings of the second throat in order to determine the optimum settings. For these tests a cone-cylinder model with 1% blockage was mounted in the test section.

An example of measured variation of  $P_{0_{min1}}$  and  $P_{0_{min2}}$  with second throat to test section area ratio  $A_2/A_{ts}$  at Mach 3.0 is plotted in Fig. 3. All pressure values are normalized by  $P_{atm}$ . The optimum second throat settings determined for various Mach numbers are plotted in Fig. 2, together with the theoretical second throat area as given by<sup>(6)</sup>. The difference between the measured and the theoretical optimum, together with the difference between the startup and the shutdown minimum pressure indicate that the geometry of the test section and the diffuser and the boundary layer development is such that a non-optimum second throat is unintentionally formed at the exit of the test section even when the choke flaps are not used.

The minimum startup and operating pressures, with optimum second throat and without the second throat, are given in Fig. 1. It can be seen that, by optimizing second throat size, a significant reduction of startup minimum pressure was achieved at higher Mach numbers.

In order to utilize the operating pressures between  $P_{0_{min1}}$  and  $P_{0_{min2}}$ , a so called 'hard startup' strategy was proposed by the wind tunnel designers and implemented in the control system: at the beginning of the run  $P_0$  was raised above  $P_{0_{min1}}$  for the particular Mach number until the supersonic flow was established, and then lowered to desired value between  $P_{0_{min1}}$  and  $P_{0_{min2}}$ .

### Transient Loads

Recordings of transient loads were made on several missile-shaped models of various shapes, lengths and cross-sections, the first one being a 160mm dia. cone-cylinder with 12.5° cone angle and length of 583mm, also used in measurements of minimum operating pressure. Another one was the AGARD-B calibration model with 116mm body diameter.

Forces and Moments: Forces and moments were measured by Able (Task) six-component internal strain gage balances with load ranges appropriate to the model tested. Several balances were used, of 1.5" (MkXXV), 2" (MkXVIII, MkXXI, MkXXXV) and 2.5" (MkXXV) diameter.

Balance bridge outputs were connected to the wind tunnel data acquisition system. In order not to interfere with custom measurements where low-pass filters with much lower cut-off frequencies were desired, the parallel 'unfiltered output' of the analog input (PPSF) cards was used beside the filtered one, and these unfiltered signals were led through additional low pass filters with 150Hz cut-off to a second analog multiplexer and D/A converter (BAMX). Sampling rates varied from test to test, but were always in the 200-500 samples/channel/s range.

Flow visualisation: In the cone-cylinder and AGARD-B tests Schlieren flow visualization was performed. A three-colour-filter Schlieren apparatus of Töpler type was used and recordings were made using a 50 frames/second 16mm cine camera.

To enable correlation of cine recordings and data recorded by the DARS, a provision was made to display synchronizing signals in the field of view of the Schlieren apparatus. To this end the vacuum-fluorescent display of a BCD digital counter was installed in the receiving end of the Schlieren, and with appropriate optics the image of the display was inserted in the field of view. The counter was triggered by impulses generated in each data sampling cycle by the analog output section of the DARS. In this manner the numbers displayed on the cine recordings directly corresponded to the ordinal numbers of data samples taken on each channel. Since the ratio of camera speed to sampling rate was not 1:1, cine frames were taken at intervals of approximately 10 samples.

Pressure distribution: Since the first measurements of forces and moments showed unusually high lateral transient loads, it was decided to measure, in parallel to measurements of forces and moments, pressure distribution on a wind tunnel model, in order to get a better insight in the phenomenon. Mechanical scanners could not be used, of course, because of the high scanning rates necessary, and discrete pressure sensors could not be connected directly to the DARS, because it was im-

possible to pass the necessary cabling for more than one transducer through the balance and sting. Therefore, it was decided that signals from pressure transducers in the model should be electronically multiplexed in the model, by a device that should not require more than six wires for connection to the DARS. For this purpose, a miniature solid-state voltage scanner<sup>(13) (14)</sup> was developed and built in the VTI, with the following characteristics:

Dimensions: 60 × 60 × 25mm  
Input channels: 16, differential  
Input, full scale: ± 100mV, differential  
Output, full scale: 1.5V, differential  
Excitation: 12V DC, 3mA  
Scanning rate: up to 20000/s  
Addressing: sequential (step+reset)  
Connection to DA system: six wires

To minimize sensibility to electrical noise, differential multiplexing and amplifying is used in the scanner, and the step/reset input is optically isolated from the analog part.

The scanner connects to 16 Druck PDCR42 differential pressure transducers in the model. The transducers are connected, with the tubing of minimum length, orifices along the upper, lower, left and right hand sides of the model.

The analog output of the scanner interfaces directly to analog input card (PPSF) of the DARS. Sensor addressing and synchronizing with other data acquisition channels is accomplished by a simple interface connected to a digital input card (PDID) of the same system. The interface contains a 4-bit counter triggered by the 'strobe' signal from the PDID card which is activated each time the DARS reads the PDID. The output of the counter is connected to the digital input lines of the PDID, in order to record the active sensor address. The 'strobe' signal is led through the output driver to trigger a counter in the scanner. To check synchronisation in case of electrical noise, a 'reset' signal is also sent to the scanner each time the counter sets the address 0000.

To operate the scanner, the DARS is set in such a manner to read both the analog data from the scanner and the digital data from the interface 16 times in each data sampling cycle. In this way, there is a 1:1 correspondence between samples from each pressure transducer, samples from the internal balance in the model, and the output of the counter in the Schlieren receiving end.

The first pressure measurements were made with a cone-cylinder model described previously. Because of the limited space available in the model, only two pressure transducers were used, the first one measuring pressure difference between the upper and lower sides of the model cone, and the other one measuring the lat-

eral pressure difference. Base pressure was also measured. Balance and pressure transducer data, together with Schlieren cine recordings were taken.

Another, larger, cone cylinder model, with 125mm diameter and 1100mm length was built to accommodate 16 pressure transducers. Unfortunately, just prior to the beginning of tests with the new model, a malfunction caused the wind tunnel system to be inoperative for some time, and afterwards, because of other scheduled tests, the measurement of transient pressures was postponed to some future time and, has not, as yet, been performed.

### Data Analysis

Flow visualisation recordings showed that there are two types of startup transient phenomena in the T-38 wind tunnel. The first one occurs at Mach numbers below 2.5 and it is characterized by the absence of strong shock waves, with relatively large areas of continuous pressure gradients (Fig. 9). At Mach numbers 2.75 to 4, a shock wave system develops (Fig. 10), with strong oblique waves usually generated on the lower plate of the flexible nozzle. The oblique shock waves often oscillate forward and backward for some time in the test section, at a frequency of about 12Hz. From the angle of the shocks, flow deflections of  $15^\circ$  to  $22^\circ$  in the vertical plane were deduced (this agrees quite well with estimates in<sup>(2)</sup>). Establishing of a supersonic flow on only one side of the model was recorded in some instances.

During run shutdown, the oblique shock waves were not recorded by the Schlieren, and transition from the supersonic to subsonic air velocities occurred very fast (in 20ms to 40ms). The transducer measuring lateral pressure difference on the model recorded, in some runs, pressure peaks that could be attributed to the oblique shock generated on the side wall and thus invisible by Schlieren. In some instances short duration establishment of a supersonic flow at reduced Mach number was deduced from shock waves appearing on the model (from Mach 3.5 to Mach 2.1; from Mach 3.0 to Mach 1.8)

Measurements of forces and moments show high dynamic transient loads (Fig. 5). At Mach numbers below 1.75 these loads are not significant. In the Mach number range 1.75 to 2.5 transient loads become higher with increasing Mach number, but still not very severe. At Mach numbers between 2.5 and 3.0 the magnitude of transient loads rises dramatically, and then remains more or less constant up to Mach 4. Generally, shutdown loads are higher and longer lasting than startup transients. Besides the expected normal loads, high axial and side forces were recorded, as well as very high pitching and yawing moments. Maximum recorded loads varied as much as 40% from run to run for the same flow

conditions.

Axial force measurements show that in the startup phase the model is subjected to two strong axial shocks immediately following each other. The first shock is towards the tail of the model, and followed by a shock of about the same intensity in the opposite direction. In the shutdown phase the situation is reversed, the load acting first in the upstream direction. Schlieren recordings and pressure measurements confirmed the proposition that these shocks occur when the nose of the model is in the region with an established supersonic stream, and the base of the model is in the subsonic region, while the shock waves travel along the length of the model. It was found that models of small length-to-diameter ratio were more sensitive to these loads. Because the transient shock waves, as mentioned earlier, often oscillate for some time in the test section, a short model can sometimes experience sustained forward-backward shocks (Fig. 5). It was found that the standard conical coupling of balances to the sting with two or four tightening screws is not adequate for such loads. In some of the tests the balance got loose, deforming the tightening screws.

Transient loads in the vertical plane (i.e. normal force and pitching moment) are characterized, at lower Mach numbers, by almost random oscillations, while, at Mach numbers above 2.50 there are several strong shocks in the startup phase, caused, as showed by the Schlieren recordings and pressure measurements, by the passage of an oblique shock wave over the model. After the initial shock, which was found to be usually acting upwards (related to the oblique shock wave generated from the lower plate of the flexible nozzle), the oscillations are slowly damped (Fig. 5). In the shutdown phase, distinct shocks caused by oblique waves were not recorded.

Side force and yawing moment measurements were harder to explain. Lateral loads were at least as high as the loads acting in the vertical plane, but no matching phenomena was detected in Schlieren recordings or pressure distribution measurements (Fig. 5). While the transducers measuring the pressure difference between the upper and lower sides of the model recorded pressure loads of the order of magnitude of 1bar, the measured lateral pressure differences were much smaller. The shutdown lateral loads were even more unexpected. Pressure peaks that probably corresponded to shock waves generated on a side wall were recorded in some runs, but could not account for the amplitude and duration of the transient loads. Moreover, it was found that violent lateral loads were recorded at the instants when the flow around the model was still completely supersonic. Such loads occurred even in the steady flow conditions when the stagnation pressure was between the starting minimum operating pressure  $P_{0_{min1}}$  and the shutdown minimum pressure  $P_{0_{min2}}$ .

The conclusion concerning the lateral transient loads was that these were not, for the most part, caused by flow phenomena in the test section, but, rather, by flow disturbances acting on the model support system, especially its vertical strut which has a large (about 2m<sup>2</sup>) lateral projected area. The proposition is made that shock waves are located in this area when the pressure ratio is favourable, and cause the whole model support to vibrate violently. Thus, lateral model loads would appear to depend mostly on model's inertial and not aerodynamic characteristics. Unfortunately, the layout of the model support strut is such that pressure transducers can not be easily installed there to confirm the proposition by actual pressure measurements.

The recorded transient forces and moments were normalized by minimum startup and shutdown stagnation pressures and model projected areas as suggested in <sup>(3)</sup> <sup>(4)</sup> to obtain the transient load coefficients for the axial, side and normal forces:

$$C_{A_s} = \frac{R_A}{S_x P_{0_{min}}} \quad (1)$$

$$C_{Y_s} = \frac{R_Y}{S_y P_{0_{min}}} \quad (2)$$

$$C_{N_s} = \frac{R_N}{S_z P_{0_{min}}} \quad (3)$$

The coefficients were compared (Fig. 4) to estimates made by both the 'normal shock method' (eqn. 4):

$$C_{*s} = \frac{7}{6} \cdot \frac{(M^2 - 1)}{(1 + 0.2 \cdot M^2)^{3.5}} \quad (4)$$

and the modification of it suggested by Maydew (eqn. 5) to account for model wing-to-total area ratio  $S_l/S_t$ , as cited in <sup>(4)</sup>:

$$C_{*s} = \frac{7}{6} \cdot \frac{(M^2 - 1)}{(1 + 0.2 \cdot M^2)^{3.5/\beta}} \quad (5)$$

where  $\beta$  is an empirical factor, calculated as:

$$\beta = \frac{3}{2} \left( \frac{M - 1}{M} \right) \left( 0.9 + 0.1 \cdot \frac{S_l}{S_t} \right); M \leq 3 \quad (6)$$

$$\beta = 0.9 + 0.1 \cdot \frac{S_l}{S_t}; M > 3 \quad (7)$$

The agreement between the estimate and the measurements was best for the normal force, especially referring to the Maydew's modification. The agreement was not so good for the axial loads, which was to be expected, because the mathematical model was not appropriate for the load acting in this direction. The 'normal shock' estimate seems better suited to axial loads. Both methods overestimated transient loads below Mach 2.

#### Empirical Estimate of Transient Loads

Tests show that transient loads in the T-38 wind tunnel are so high that it is necessary to make an estimate

of them for every model to be tested at Mach numbers above 2. It was decided that estimation by 'normal shock method' was not adequate for the T-38 wind tunnel. Pitching, yawing and rolling moments could not be estimated in this way. Also, because lateral loads seem to have a cause not directly related to model aerodynamics and geometry, side force estimates were not reliable. To express transient load as a certain multiple of stationary test loads, as was done in some wind tunnel facilities, seemed even more indeterminate.

Therefore, an approach used by the Boeing Company<sup>(9)</sup> for the BSWT facility was adopted. The transient loads are expressed essentially as differential pressures acting on the model. Normalized values of the transient forces  $k_x \dots k_z$  were determined by normalizing the maximum recorded loads with model projected frontal, plan or profile area, while the transient moments  $k_l \dots k_n$  were normalized both by appropriate areas and by model wing span or length (the implied assumption is that  $S_l/St$  does not vary much for typical missile models and so should not be considered as a variable):

$$k_x = \frac{R_{A_{max}}}{S_x} \quad (8)$$

$$k_y = \frac{R_{Y_{max}}}{S_y} \quad (9)$$

$$k_z = \frac{R_{N_{max}}}{S_z} \quad (10)$$

$$k_l = \frac{M_{x_{max}}}{B \cdot S_x} \quad (11)$$

$$k_m = \frac{M_{y_{max}}}{L \cdot S_x} \quad (12)$$

$$k_n = \frac{M_{z_{max}}}{L \cdot S_x} \quad (13)$$

The actual transient loads that can be expected on the particular model are derived from the inverse relations:

$$R_A = k_x \cdot S_x \quad (14)$$

$$R_Y = k_y \cdot S_y \quad (15)$$

$$R_N = k_z \cdot S_z \quad (16)$$

$$M_x = k_x \cdot S_x \cdot B \quad (17)$$

$$M_y = k_x \cdot S_y \cdot L \quad (18)$$

$$M_z = k_x \cdot S_z \cdot L \quad (19)$$

Figure 6 shows the values of estimates  $k_x \dots k_n$  together with normalized values of measured transient loads for several missile models. While these data do not take into account the inertial characteristics of the model, which are important keeping in mind the nature of the lateral loads, it is felt that it can be used to get a reliable estimate of maximum transient loads, valid, of course, only for the missile shaped models and the T-38 facility. Models to be tested are to be designed with adequate safety factors having in mind the obtained estimates.

An improved estimate of transient loads for each model to be tested at high Mach numbers is obtained by the procedure of testing such models first at Mach numbers 1.75, 2.00 and (if possible) 2.25, regardless of the actual test programme, in order to record the actual loads. Transient loads at these Mach numbers are not very severe, so it is almost certain that every model or balance used can withstand them. The normalized transient loads are then compared to the data in Fig. 6, and extrapolated to higher Mach numbers. While, at this stage in a test programme, it is too late to modify model design, this check can at least prevent the model or the balance from being damaged if previous estimates of transient loads were erroneous.

#### Reduction of Transient Loads

Several attempts were made to reduce the transient loads. Major modifications of the wind tunnel (such as installing ejectors to reduce diffuser pressure, removing diffuser baffles and silencer, or installing proximity plates) were quickly ruled out because of the cost and time involved. Therefore, it was attempted to reduce the transient loads by other means.

The first approach was proposed by the tunnel designers and required installation of wedge-shaped shock generators on the left and right hand side walls of the test section. According to some references, these 'precursor' shock generators were supposed to stabilize the flow and improve supersonic diffusion. However, measurements showed that these additions had absolutely no effect, except for the barely discernible change of the minimum operating pressure. This attempt was therefore abandoned.

Since there is a significant upward flow deflection behind the oblique startup shock wave, it was attempted to reduce the transient loads by pitching the model to a small negative angle. From several tests with the conecylinder model, an optimum pitching angle of about  $-7^\circ$  was determined. Startup normal loads were reduced in this way by about 40%, but, of course, lateral loads were not affected, and neither were the shutdown transient loads. Therefore, this approach is not very useful.

Plots of traverse transient load vector directions (Fig. 8) show that the largest transient loads are mostly restricted to the vicinity of the vertical and horizontal planes. Since the flexure elements for normal and side forces and/or moments in the internal strain gage balances are, in the majority of runs, also oriented in the vertical and horizontal planes, most of the time during the transients only one pair of flexures receives the load. Several tests were made with model rolled to  $45^\circ$  (the particular balance used having equal load capacities in vertical and lateral plane), and indeed, significant reduction of maximum transient loads acting on the balance (about 25%) was detected. However, only the balance

can be protected in this way, the model and the sting still sensing the same loads. Besides, relatively slow roll rate of the support mechanism ( $40^\circ/\text{s}$ ) makes this method unusable for tests at flow conditions in which only a short run time is available and the model is to be tested at roll angles other than optimum for reduction of the transients.

Another attempt was made to reduce the transients acting on the balance by limiting the clearance between the aft part of the model and the support sting to a value slightly larger than the sting deflection expected during the tests at steady flow conditions. In this way part of the transient loads was supposed to transfer directly to the sting, bypassing the balance. Tests with a missile model showed that transient pitching and yawing moments can be reduced in this way by about 50% (Fig. 7), while normal and side forces are slightly increased. The drawback of this approach lies in the difficulty to judge the necessary model-balance clearance before the actual wind tunnel run. Also, only the balance is protected in this way, not the model and the sting.

The tests show that for high Mach number runs the balance should be located, whenever possible, at, or slightly forward of the centroid of the projected model plan (or profile) area, because in this way the additional pitching and yawing moments imposed on the balance, and also the support sting deflections are minimized.

It showed that model size optimum for testing at lower speeds (about 0.5% blockage, model diameter not more than 110mm, model length not more than 1500mm) was too large for supersonic tests because of the large transient loads induced. Transient yawing and pitching moments, which are the most critical, are scaled with model size cubed, while the balance or sting load capacity is roughly proportional to model size squared. Therefore the load/capacity ratio is more favourable for smaller models and the recommended model size for future tests is reduced to about 60mm maximum diameter and maximum length of about 1000mm.

It was felt that the range of internal Able balances available at the Institute was not suitable for tests where high transient loads were expected. Since the Aeronautical Institute has mastered the design and production of high quality monoblock strain gage balances, three balances more convenient for supersonic missile tests were designed and their manufacture initiated. These balances are characterized by large length-to-diameter ratio, thus having high moment loading capacities relative to normal and side force capacities. Also, high impedance strain gages are to be used, making it possible to get useful signals from very stiff flexure elements. The smallest balance has a 38mm diameter with 3kN, 300Nm load ranges both for normal and side loads, the medium one has 40mm diameter with a 6kN, 600Nm load range, while the largest balance has a 45mm di-

ameter and a 15kN, 1800Nm load range. Because of the described problems with the conical balance-to-sting coupling, the largest balance's mating cone will not be tightened to the sting with four screws, but rather with a nut with thread and counterthread, located around the joint of the balance and the sting. The smallest one of these balances has been finished and calibrated, and is being routinely used for testing models at Mach numbers up to 2.5.

Having in mind the recommended model geometry and balance positioning, and also the newly designed balances, the appropriate model support stings are being built, with length kept to a minimum that will not significantly affect base pressure measurements, so that as high as possible stiffness and load capacity can be obtained.

### Conclusions

Minimum operating pressure of the T-38 wind tunnel is certainly higher than designed. The method of reducing the minimum operating pressure by means of a second throat was successful but the 'hard startup' procedure can not be used when measurements of forces and moments are performed because of the strong lateral oscillations originating in these conditions at the model support strut.

Transient loads acting on the model are also higher than in the design estimate, but this is mostly a consequence of high minimum operating pressure, because measured transients normalized by minimum pressure agree well with theory, except for lateral loads which are mostly a consequence of too low lateral stiffness of the model support strut. Further tests are needed to resolve the effects of model's inertia on transient loads.

Since any extensive modifications of wind tunnel structure (such as redesigning the diffuser or the model support strut) are out of the question, the present situation has to be lived with, and the high Mach number range of the T-38 can be utilized by limiting model size, especially length, and using the appropriately designed balances and support stings. This means, however, that very slender models, with length to diameter ratio higher than about 16:1 are not suitable for tests at high Mach numbers in the T-38.

The simple method of estimating transient loads by multiplying the empirically obtained load coefficients by projected model areas and lengths can be used to estimate the transient loads for models to be tested at high Mach numbers. By pitching the model to a certain small negative angle, rolling it to 45°, and by controlling the clearance between the model and the support sting, a reduction of transient loads by about 50% is possible in some cases.

### References

- 1 B. Medved, G.M. Elfstrom: "The Yugoslav 1.5m Trisonic Blowdown Wind Tunnel"; AIAA Paper 86-0746-CP, 1986
- 2 K.G. Winter, C.S. Brown: "Loads on a model during starting and stopping of an intermittent supersonic wind tunnel"; RAE Technical Note No. Aero.2453, May 1956
- 3 S.L. Kinsolving, R. Jackson: "Starting Loads in an Intermittent Supersonic Wind Tunnel"; AEDC-TN-59-6; Jan. 1959
- 4 R.C. Dixon: "Estimates of Starting and Stopping Loads in the N.A.E. 5 foot Trisonic Wind Tunnel"; NAE, HSA-23; Feb. 1966
- 5 J.R. Digney: "An Update on Supersonic Starting and Stopping Loads in the 5-ft Wind Tunnel"; NAE HSA-156; Dec. 1977
- 6 A.H. Shapiro: "The Dynamics and Thermodynamics of Compressible Fluid Flow"; The Ronald Press Company; 1954
- 7 "Proximity Plates: Yes or No?"; DSMA Inc. Design Report 4001/07 #1; Ma. 1977
- 8 "Estimation of Break-down (min.) Pressure Ratios (Yugo 1.5m)"; DSMA Inc. Design Report 4001/01 # 9; July 1978
- 9 The Boeing Company: "Shock loads"; D2-22871; section 2
- 10 Đ. Vuković: "Ispitivanje prelaznih opterećenja u aerotunelu T-38" (Testing of transient loads in the T-38 wind tunnel); Aeronautical Institute Žarkovo, V3-2404-I; Jan. 1986
- 11 Đ. Vuković: "Ispitivanje prelaznih opterećenja u aerotunelu T-38 koničnim modelom i aerovagom Ejbl MkXXV" (Testing of transient loads in the T-38 wind tunnel with a conical model and Able MkXXV balance); Aeronautical Institute Žarkovo, V3-2464-I-EA; July 1987
- 12 Đ. Vuković: "Ispitivanje mogućnosti smanjenja prelaznih opterećenja pri ispitivanjima modela na visokim Mahovim brojevima u aerotunelu T-38" (Testing of a possibility of reducing the transient loads when testing models at high Mach numbers in the T-38 wind tunnel); Aeronautical Institute Žarkovo; V3-2653-I-EA; May 1991
- 13 M. Guberinić: "Primena analognih elektronskih multiplexera u aerotunelskim ispitivanjima" (Application of analog electronic multiplexers in wind tunnel tests); The proceedings of the 8th Yugoslav Congress of Aerospace Sciences; Mostar 1987
- 14 Đ. Vuković: "Integracija elektronski skaniranih davača pritiska sa aerotunelskim sistemom za prikupljanje podataka" (Integrating electronically

scanned pressure sensors with wind tunnel data acquisition systems); The proceedings of the Aeronautics '93 meeting; Belgrade University; Belgrade 1993

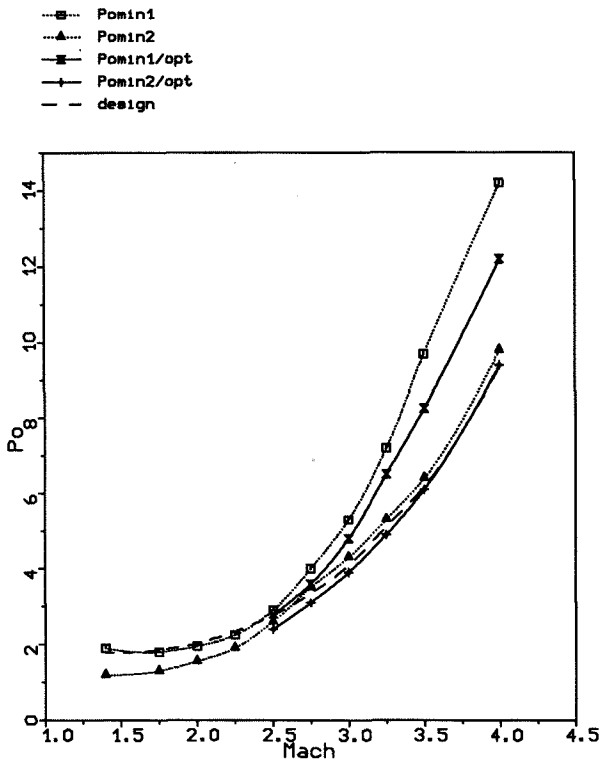


Fig.1: Minimum operating pressure

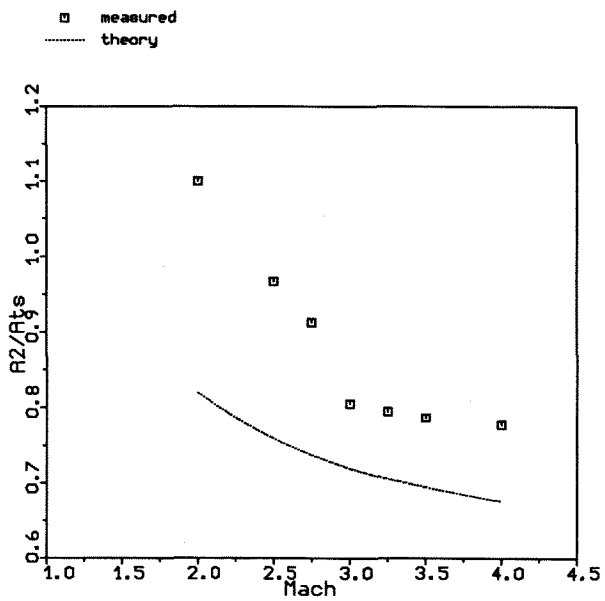


Fig.2: Optimum second throat settings

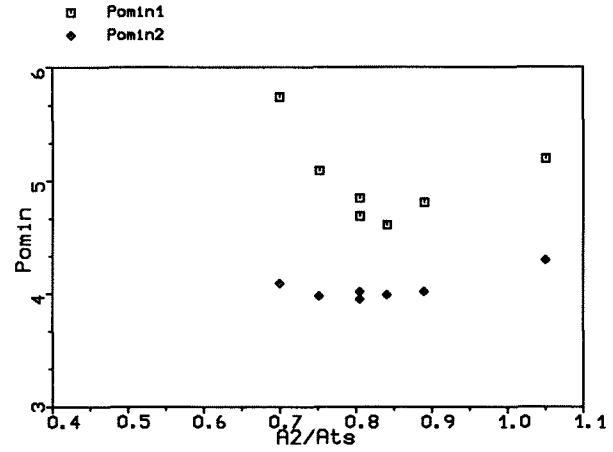


Fig.3:  $P_{0_{min}}$  vs. second throat settings; Mach 3

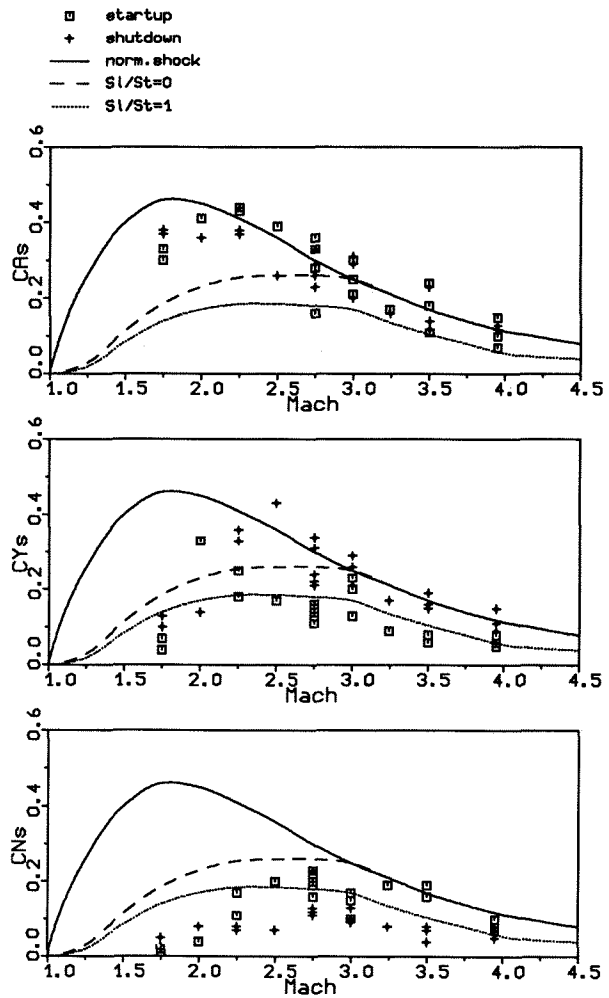


Fig.4: Transient load coefficients; cone-cylinder model



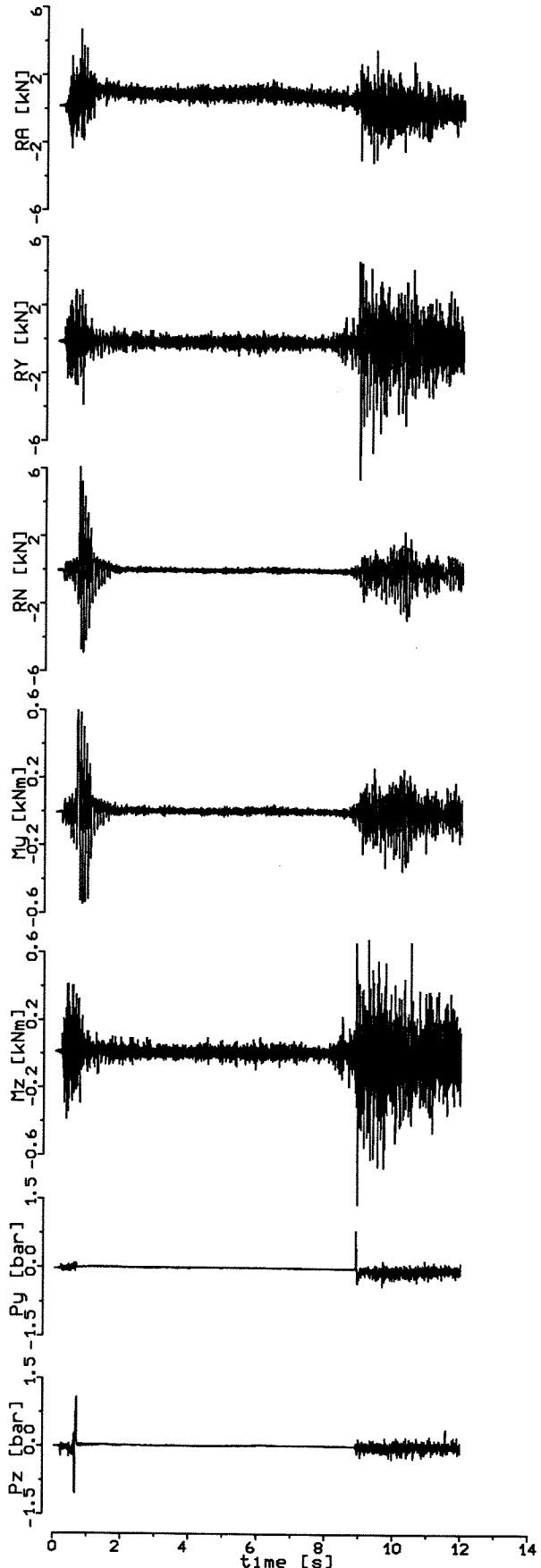


Fig.5: Recordings of  $R_A \dots M_z$ ;  $P_y$  and  $P_z$  during a run; cone-cylinder model;  $\alpha=0$ ; Mach 3.5

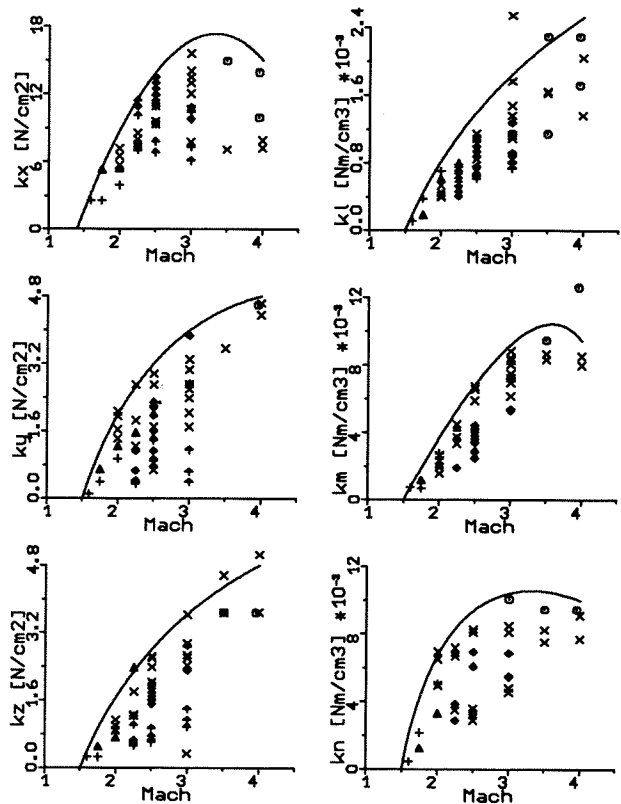


Fig.6: Estimates of normalized transient loads compared to measured loads

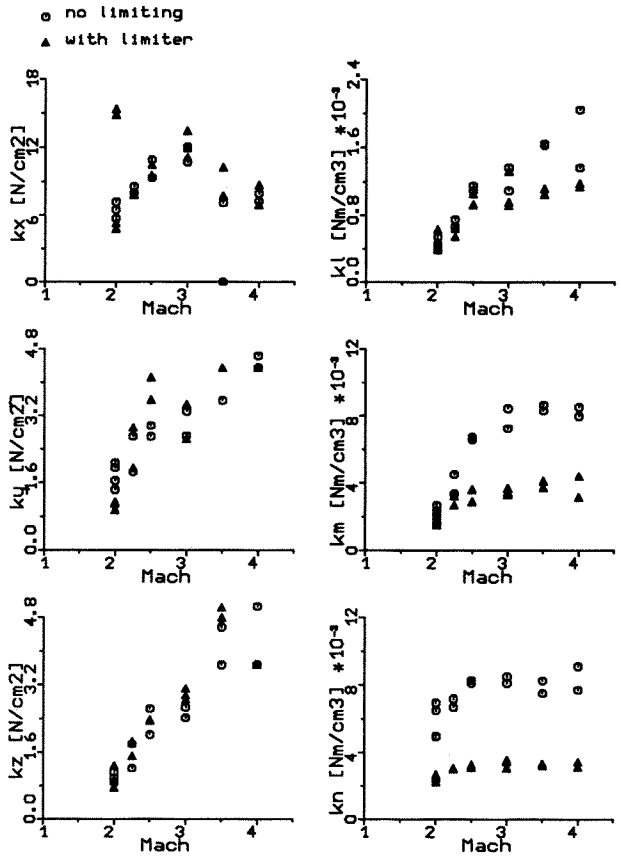


Fig.7: Effect of limiting model-sting clearance

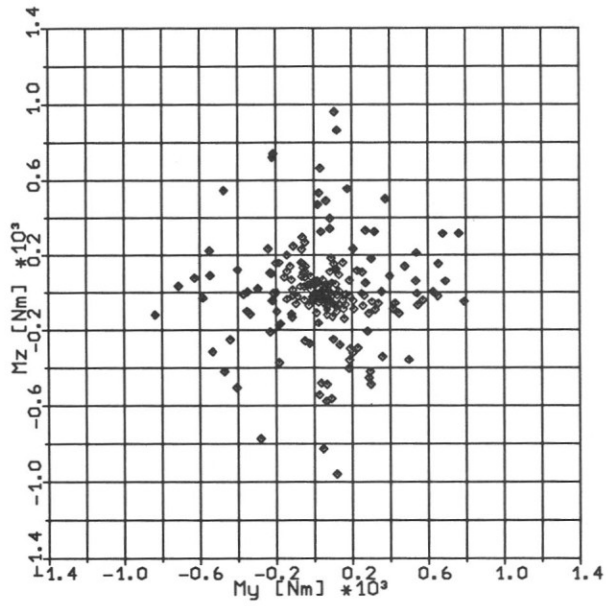


Fig.8: Directional distribution of moment load vectors; Mach 3.5

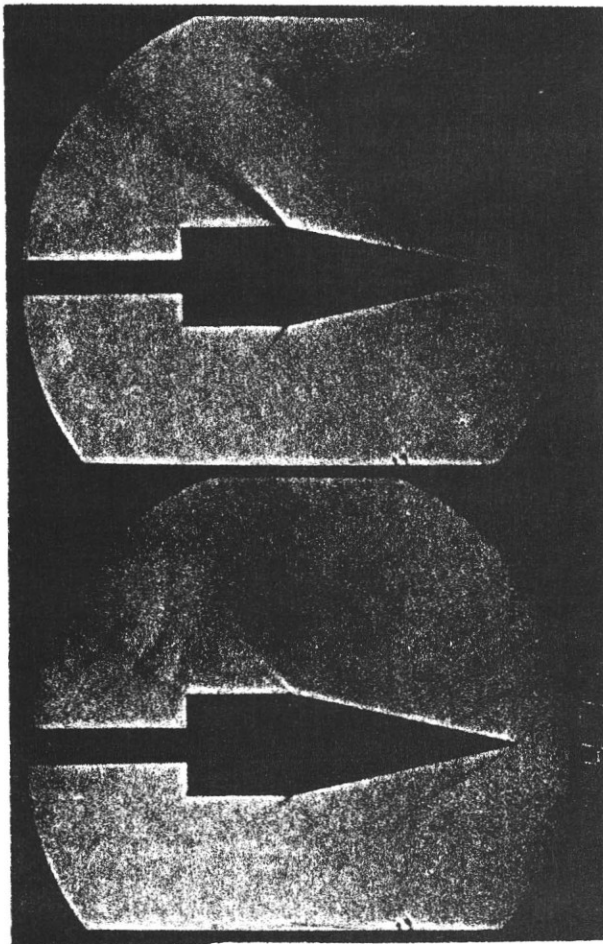


Fig.9: Cine recordings of transient phenomena; cone-cylinder model; Mach 2.5

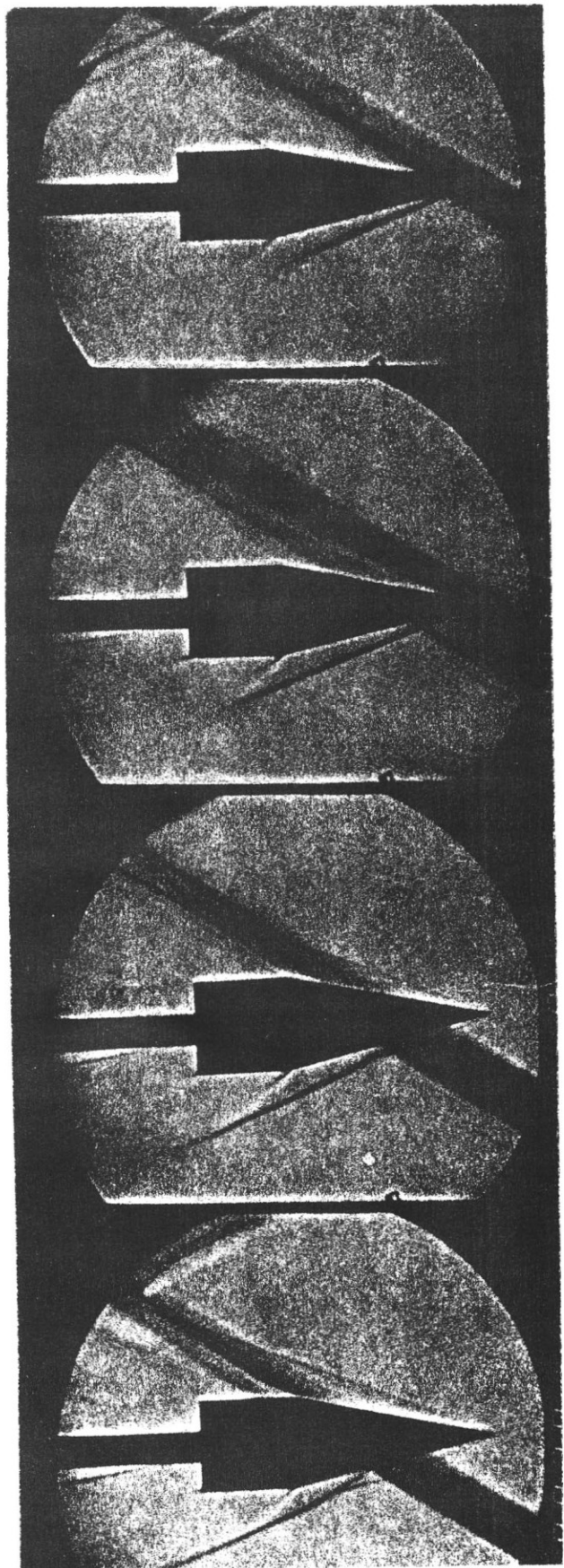


Fig.10: Cine recordings of transient phenomena; cone-cylinder model; Mach 3.5